Verifying the Compton Scattering Formula and Observing the Klein-Nishina Relation

Elisa Jacquet, An Vuong, Alev Orfi

McGill University Department of Physics

Supervisor: Prof. Brunner & Prof. Sankey

April 8, 2019

Abstract

Today, light is known to possess characteristics of both waves and particles, a property called wave-particle duality. However, in the early 1900s this was still a contested theory. In 1923, Arthur Compton famously demonstrated that the particle-nature of light was necessary to explain scattering of photons off targets. This effect is known as Compton scattering and is still one of the most well-known experiments that show evidence supporting the quantum mechanical interpretation of light as a particle. In this report, photons from a ^{137}Cs source were scattered of an Al target and analysed to reproduce the results observed by Arthur Compton. We verified Compton's relation by using our data to calculate the electron's mass. It was found that the electron's mass is $(9.4 \pm 0.3) \cdot 10^{-31}$ kg, which is in agreement with the literature value of $m_e = (9.109\ 383\ 56\ \pm 0.000\ 000\ 11) \cdot 10^{-31}$ kg. Another goal of this experiment was to verify the Klein-Nishina formula qualitatively, and thus show the importance of relativistic effects in Compton scattering. We were able to recover a linear fit between our measured counting rate and the theoretical prediction for counting rate as a function of angle. This linear relation had a $\chi^2 = 1.5 \pm 1.0$, supporting the Klein-Nishina formula.

Contents

1 Introduction

Classically light is described as alternating electric and magnetic waves. In the twentieth century, there was an increase of experimental evidence suggesting a particle nature of light [1]. Compton scattering is among the phenomena which demonstrated the particle attributes of light [1]. This report explores the fundamental properties of Compton scattering, demonstrating experimentally the validity of this theory.

Compton scattering is the scattering of a photon off a charged particle (in this case an electron). It is found experimentally that scattered photons have longer wavelength than those incident upon the target [2]. In particular, the wavelength of the scattered light varies with the scattering angle. This shift in wavelength is described by the Compton relation [2],

$$\Delta\lambda = \frac{h}{m_e c}(1 - \cos(\theta)). \tag{1}$$

Here λ is the wavelength of the light, m_e is the rest mass of the electron, θ is the scattered angle, h is Planck's constant and c is the speed of light. This formula can be expressed in terms of energy, E, using the Planck-Einstein relation,

$$E = \frac{hc}{\lambda}. \tag{2}$$

With this, the Compton relation becomes

$$\frac{1}{E_i} - \frac{1}{E_f} = \frac{1}{m_e c^2}(1 - \cos\theta). \tag{3}$$

Where E_f is the energy of the scattered photons, and E_i is the energy of the photons incident upon the electron. This change in wavelength (or energy) is explained by modelling photons as particles. The scattering can then be analyzed as an elastic collision between photons and electrons [2]. The Compton relation is retrieved by applying conservation of energy and momentum to this system. The energy of the electron after the collision is given by the relativistic energy-momentum relation [3],

$$hf + m_e c^2 = hf' + \sqrt{(p_e c)^2 + (m_e c^2)^2}. \tag{4}$$

Here f is the frequency of the light before the collision, f' is the post collision frequency and p_e is the final momentum of the electron. The conservation of momentum is a vector relation,

$$\mathbf{p_e} = \mathbf{p}_\lambda - \mathbf{p}_{\lambda'}. \tag{5}$$

Here, $\mathbf{p_e}$ is the momentum acquired by the electron, $\mathbf{p}_\lambda$ is the momentum of the incident photon and $\mathbf{p}_{\lambda'}$ is the momentum of the scattered photon. Equating $\mathbf{p_e}$ from equation 4 and equation 5 gives rise to the Compton relation [3]. As the Compton relation is a direct result of the particle nature of light,it was essential to the development of quantum physics in the early 1900s [1].

It is also of interest to define the probability that a photon will be scattered at a given angle. Mathematically, this means calculating the differential cross-section $d\sigma/d\Omega$. Theoretically, the differential cross-section is given by,

$$\frac{d\sigma}{d\Omega} = \frac{\text{Number of particles detected at a given angle per unit solid angle}}{\text{Number of particles incident per unit area}}. \tag{6}$$

Classically - that is without taking into account the effects of relativity - the differential cross-section is given by Thomson's formula

$$\frac{d\sigma}{d\Omega} = r_0^2 \frac{(1+\cos^2\theta)^2}{2}. \tag{7}$$

Where θ is the angle from the incident ray, and $r_0 = 2.818 \times 10^{-13}$ cm is the classical radius of an electron [3]. However, for incident photons of high energy (X-ray or γ-ray) equation 7 no longer holds. In order to accurately describe scattering at high energy a more precise description of scattering is necessary, one which takes into account quantum mechanical and relativistic effects [3]. This description is known as the Klein-Nishina formula:

$$\frac{d\sigma}{d\Omega} = \frac{r_0^2}{2} \frac{1+\cos^2\theta}{(1+\alpha_0(1-\cos\theta))^2} \left[1 + \frac{\alpha_0^2(1-\cos\theta)^2}{(1+\cos^2\theta)(1+\alpha_0(1-\cos\theta}\right]. \tag{8}$$

Where $\alpha_0 = \frac{E}{m_e c^2}$, with E the energy of the incident photon. It is important to note here that the Thomson formula 7 is the classical limit of the Klein-Nishina formula.

This report presents an initial analysis on the phenomenon of Compton scattering. First, the quantum physical interpretation of light as a particle is verified experimentally through

the Compton relation (equation 1). Then, the importance of relativistic effects in the system is determined by demonstrating that the Klein-Nishina formula correctly models the data.

2 Experimental Set-up

In this experiment, a beam of photons is obtained from a 0.1 Ci source of ^{137}Cs. It is known that the photons from ^{137}Cs are gamma rays with energy 661.657 keV [4]. The material used to scatter these incident photons is a rod of aluminium aligned directly with the source. To detect the scattered photons, a scintillation NaI detector with a photo-multiplier is placed on a rotating disc so that the angle θ at which scattered rays are counted can be adjusted manually. Figure 1 shows this set-up, along with the position of lead blocks used to collimate the gamma ray beam. This collimation is necessary as a safety measure and as a means to minimize background noise collected by the detector.

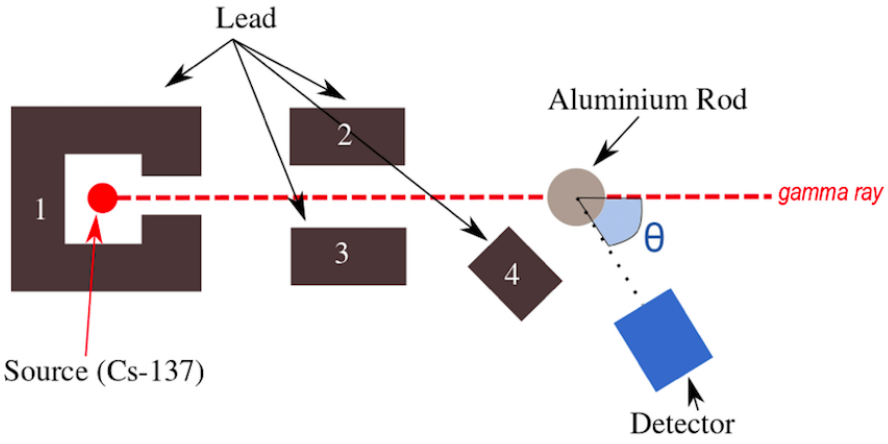

Figure 1: Experimental set-up to measure Compton scattering. Lead blocks 1-3 are used to collimate the gamma ray beam emitted from the Cs-137 source and to ensure the safety of students in the lab. Lead block 4 is positioned in such a way to minimize the detection of rays scattered by the collimators themselves (i.e. reduce background noise of detection). The angle θ is the angle at which the scattered photons are measured and is adjusted manually.

The detector ensemble is directly connected to a computer equipped with the data-collection platform MAESTRO. Through MAESTRO, the detector can be turned on and off. The set-up gives data in the form of counts per channel. Each channel corresponds to an energy so that the measurements give the number of photons as a function of energy that are incident upon the detector at an angle θ with respect to the incident beam. The relationship

between energy and channel number is determined in the calibration step of the experiment.

3 Analysis

3.1 Calibration

Calibration of the equipment was required to obtain the relation between channel number and energy of photons counted. This process was done by collecting three known γ-ray spectra from three different radioactive sources placed 10 cm from the detector: ^{22}Na, ^{133}Ba, and a weaker ^{137}Cs.

The spectra of these sources are well-documented such that it is known what energies the peaks in the γ-spectrum occur. To find a relation between energy (in keV) and channel number, it suffices to find what channel numbers each peak in the spectrum occurs at and compare this to the known energy of that peak. The energy versus channel relation is expected to be linear. Fitting this linear relationship yields the constant of proportionality between energy and channel number. This linear relationship is heavily dependent on the gain and voltage applied to the photo-multiplier/detector. For the purposes of this report, the gain will be maintained at 1.6001 and the voltage at 1000V.

A fit was performed to find the channel number of each peak. The peaks were fitted with the function described by

$$G + S + L = [e^{\frac{(x-x_0)^2}{\sigma^2}}] + [1 - (1 + e^{\frac{-(x-x_0)}{\sigma}})^{-1}] + [mx + b] + c. \tag{9}$$

Where G is a Gaussian function centered at x_0 with standard deviation σ; S is a smeared step function also centered at x_0, smeared by a factor of σ; L is a linear function with slope m and y-intercept b, and c represents a constant offset. The Gaussian function was used to describe the random distribution of counts about the maximum of the peak. The step function takes into account the Compton scattering that takes place within the detector's crystal, which is an intrinsic properties of detectors. Finally, the line and constant offset are included to model the background noise in the data - coming from back-scattering, scattering off the lead etc. A sample fit is shown in figure 2 where the fit was performed on the peak of ^{137}Cs with energy 661.657 keV [4]. Similar fits were preformed on ^{22}Na with a peak at 511.0

keV [5] and ^{133}Ba with peaks at 80.9979 keV [6] and 356.0129 keV [6]. The linear fit relating energy to channel number was then performed and is shown in figure 3. The conversion between channel number and energy was determined to be

$$\text{Channel Number} = (0.55622 \cdot \text{Energy}) - 4.685. \tag{10}$$

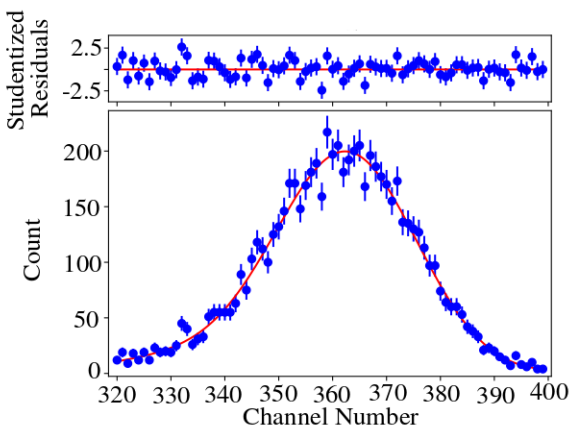

Figure 2: Sample fitting of a peak in the γ-ray spectrum of ^{137}Cs. This is the peak corresponding to the energy value of 661.6 keV. The fit gave the peak maximum to be at channel number 362.88±0.41 with a $\chi^2 = 1.04 \pm 0.16$.

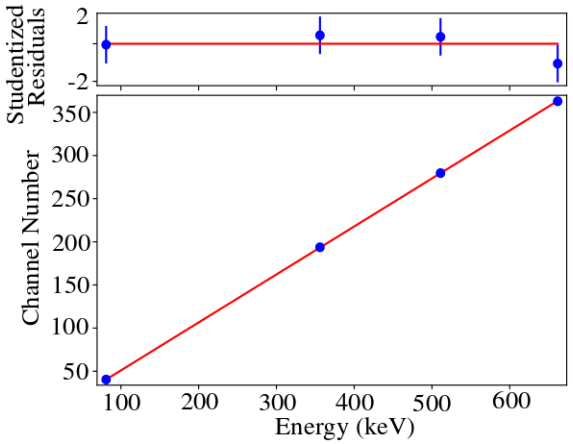

Figure 3: The plot of energy of the γ-rays observed versus channel number. Each point on this graph was obtained by finding the channel number of peaks in the γ spectra of ^{137}Cs, ^{22}Na, and ^{133}Ba. A linear relation is observed with slope of 0.55622 ± 0.00028 and a y-intercept of -4.685 ± 0.056, with a $\chi^2 = 0.7 \pm 1.0$.

3.2 Compton Scattering

With a relation between the bin number and the energy we can verify the Compton relation using equation 3. The energy of photons scattering off an aluminium rod was measured for 6 different angles. By the Compton relation, we show that the linear relationship between $(1 - \cos\theta)$ and $(\frac{1}{E_i} - \frac{1}{E_f})$, gives slope equal to the inverse of the electron's rest energy $(m_e c^2)$ within uncertainty.

In order to obtain the energy of scattered photons the peaks in the measured γ-spectra at each angle had to be processed in a similar way as in the calibration. First, the data was processed according to calibration results to give a spectrum in terms of energy. To properly

identify the peak, a background fit was also performed: at each angle, data was collected without the Al target to observe the background radiation seen by the NaI detector. The background noise was modeled by equation 9. For each angle, this background function was fixed and added to the new fitting function in the following way:

$$G + S + Background = [e^{\frac{(x-x_0)^2}{\sigma^2}}] + [1 - (1 + e^{\frac{-(x-x_0)}{\sigma}})^{-1}] + Background + c. \tag{11}$$

Here, G and S are defined in the same way as in equation 9, c is a constant offset and $Background = G + S + L$ is a fixed function based on the data obtained without the aluminum target. With this function, it is possible to fit the peak in the observed γ-spectrum and get a value of the energy of the scattered ray E_f. A sample fit is shown below for 25°, where figure 4 shows the peak fitting in the γ-spectrum obtained with the aluminium target and figure 5 shows the different functions considered in the fit plotted alongside the raw data.

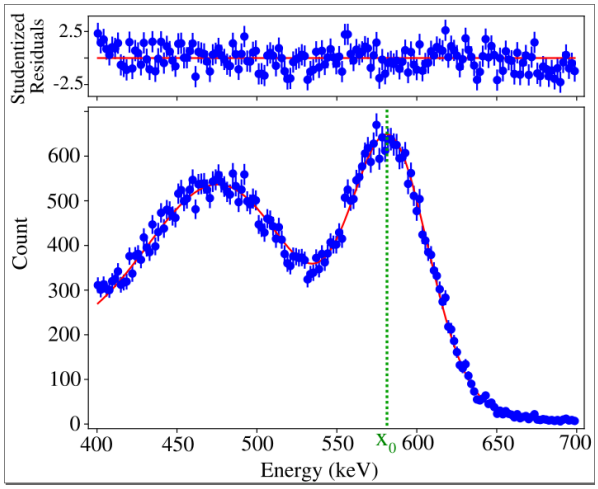

Figure 4: Sample of the fitting of the peak due to Compton scattering at 25°. The fit was performed with equation 9 and yielded a $\chi^2 = 1.14 \pm 0.11$ with 162 DOF. The peak's position, shown on the figure by the green dotted line, was found to be $x_0 = 583.65 \pm 0.26$ keV.

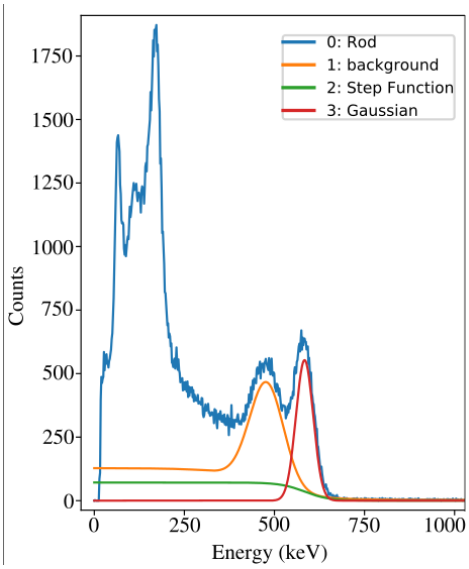

Figure 5: Four curves are shown; the raw data, the fit of the background noise, the step function characteristic of detectors, and the Gaussian curve which fits for the energy of the Compton-scattered photons.

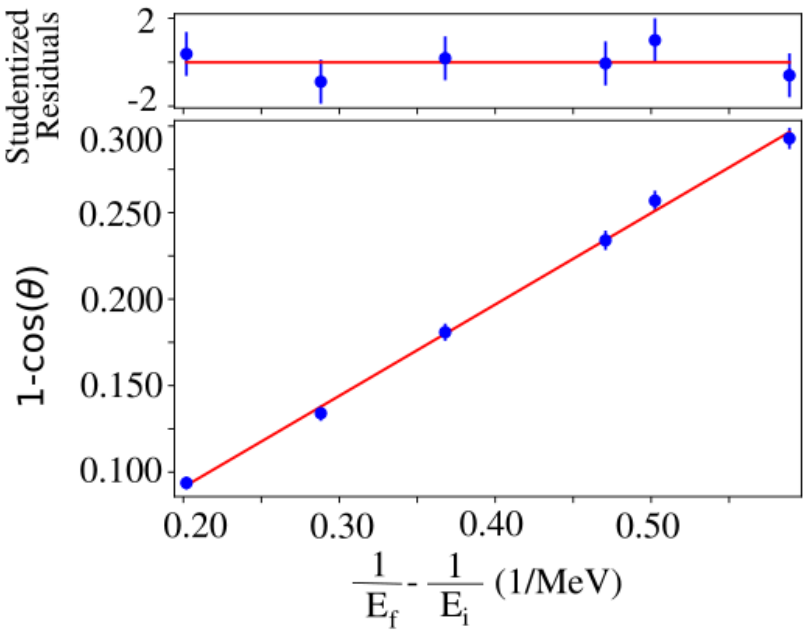

Figure 6: Experimental verification of the linear Compton relation. The slope of this line was found to be 528.0±15.0 keV. The fit had $\chi^2 = 0.58 \pm 0.71$ with 4 DOF.

Using this method, the energy of photons scattered off the Al target (E_f) was obtained for 25°, 30°, 35°, 40°, 42°, and 45°. Plotting $(1 - \cos\theta)$ and $(\frac{1}{E_i} - \frac{1}{E_f})$ for this data resulted in the plot shown in figure 6. Note that the function plotted is

$$m_e c^2 (\frac{1}{E_i} - \frac{1}{E_f}) = 1 - \cos\theta, \tag{12}$$

such that the slope obtained from the fit should be the rest energy of the electron. The linear fit gave a slope of 528.0 ± 15.0 keV. This predicts the mass of the electron to be $m_e = (9.4 \pm 0.3) \cdot 10^{-31}$ kg agreeing within uncertainty with the accepted value of $m_e = (9.109\ 383\ 56\ \pm 0.000\ 000\ 11) \cdot 10^{-31}$ kg [7].

3.3 Verifying the Klein-Nishina Formula

The Klein-Nishina Formula (equation 8) is given as a differential cross section. In this experimental setup the differential cross section is given by,

$$\frac{d\sigma}{d\Omega} = \frac{I}{(\Delta\Omega) N I_0}. \tag{13}$$

Where I is the number of scattered photons, N the number of electrons in the target, I_0 the flux density at the target, and $\Delta\Omega$ is the detector solid angle. The value of N is specific

to the material of the target and given by,

$$N = \frac{V\rho Z N_A}{M}. \tag{14}$$

Where V is the volume of the detector, ρ the material's density, Z the material's atomic number, M its molar mass, and N_A is Avogadro's number. With this relationship we have measured values for all variables in the Klein-Nishina formula excluding I_0, the flux density at the target. This value must be extrapolated through the attenuation of the beam radiation through concrete blocks. This added analysis is necessary as the detector cannot read data at 0°due to the high intensity of the radiation. The attenuation relation is given as

$$I = I_0 e^{-(\frac{\mu}{\rho})x}. \tag{15}$$

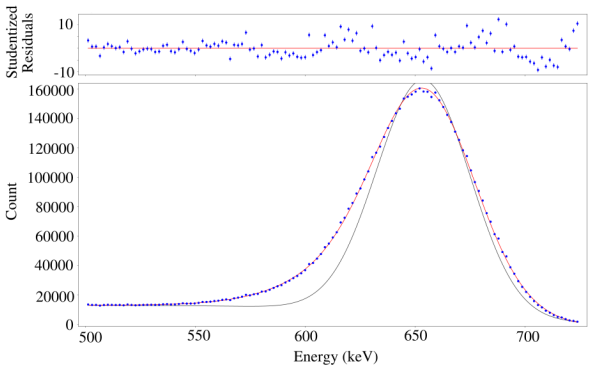

Figure 7: Sample of the fitting of the attenuation data. The fit was performed with equation 11 and yielded a $\chi^2 = 17.35 \pm 0.13$ with 117 DOF.

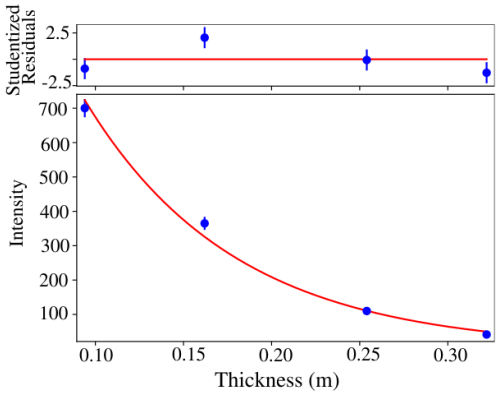

Figure 8: Exponential fit of attenuation data, yielding a $\chi^2 = 3.3 \pm 1.0$ with 2 DOF

Where I is the measured intensity, x is the thickness of the absorbing material, μ is the attenuation coefficient, and ρ the material's density. The value of $\frac{\mu}{\rho}$ is known as the mass attenuation coefficient, which is 19.7666±0.0001 for concrete [8]. Intensity data was taken for the attenuation of the radiation through 1 to 4 concrete bricks. This data proved more difficult to analyze as we no longer had stand-alone background data and Compton scattering within the blocks added additional complexity [9]. To account for this internal scattering, a skewed Gaussian was added to our fit equation [10]. With this, we obtained the the intensity

values for the four different thicknesses of absorbing material. An example of the fit, and the corresponding fitting functions seen in figure 7.

The intensity values for each block of concrete were then fitted with an exponential function. Following equation 15 this would allow the determination of I_0. The fit is shown in figure 8. Unfortunately, the mass attenuation coefficient found with this fit is 11.7 ± 0.4 which is not constant with the literature value of 19.7666 ± 0.0001 [8]. This indicates an error in our data taking or fitting. Thus for the remainder of the report we will confirm the Klein-Nishina formula qualitatively as we are unable to obtain an accurate value for I_0.

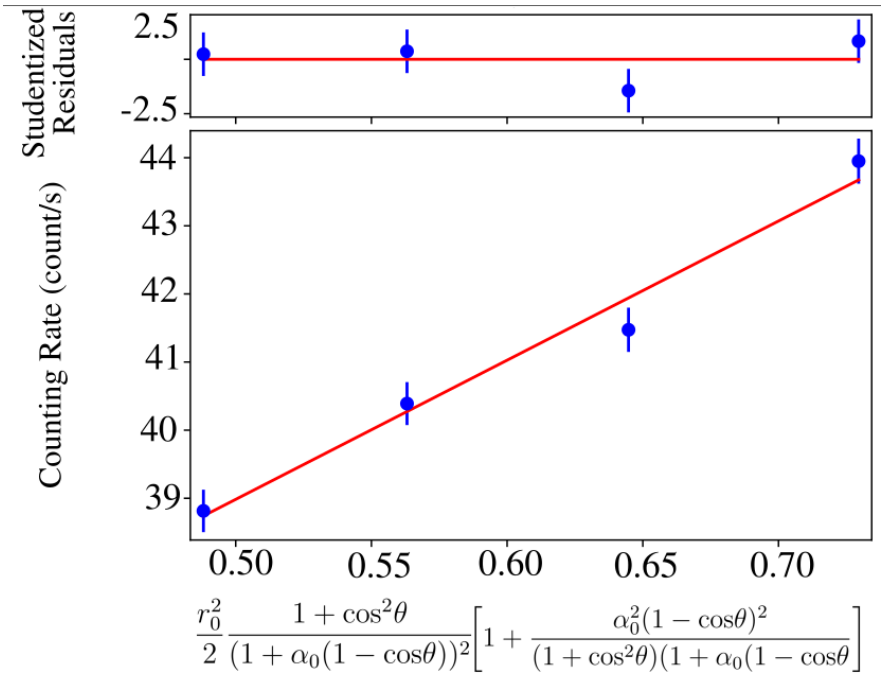

Figure 9: A linear fit of counting rate versus the value determined by the Klein-Nishina formula from the angles. A chi squared of 1.5 ± 1.0 is evaluated with 2 DOF.

To verify Klein-Nishina Formula, we proceeded on calculating counting rate (number of scattered photons per unit time). This quantity is directly proportional to the differential cross-section according to equation 8. The number of counts was calculated by integrating the peak obtained by subtracting the data before and after scattering. The counting region was determined to be the full width at half the maximum of that peak. For the sake of consistency, we chose to perform this analysis on data at 25°, 30°, 35°, 40°. A linear fit was used on the value determined by Klein-Nishina formula 8 from the angles and the counting rate. Figure 9 shows that a linear relation is presented, thus verifying the Klein-Nishina

formula.

4 Conclusion

During the twentieth century Compton scattering was one of many experiments demonstrating the particle nature of light. These experiments indicated the need for new, more general physical theories. This report demonstrates the experimental validity of the Compton relation, and thus the particle properties of light. The NaI detector was first calibrated, giving a relation between the bin number and the energy of the recorded light. This calibration was preformed by comparing the bin number and peak energy of data collected from ^{22}Na, ^{133}Ba, and ^{137}Cs. From there scattering data was analyzed for various angles with photons coming from a strong ^{137}Cs source. Data was collected without the target allowing the background effect to be modelled. The scattered data was then fitted with the sum of the background, a Gaussian, a step function and a constant off-set, giving a peak energy for each angle. With this data a value for the relativistic mass of the electron was found using the Compton relation. Our results is within uncertainty of the literature value, showing the validity of the Compton relation.

Furthermore, we were able to able verify the Klein-Nishina formula up to a proportionality constant. This demonstrates the importance of relativistic effects in this scattering model. We showed a linear relationship between the intensity values of our data and the differential cross section given by the Klein-Nishina relation. Looking forwards, it would be important to verify the Klein-Nishina formula more formally. This would require a good measurement of I_0, the intensity of the incident beam, and would demand us to re-visit our peak-fitting model.

References

[1] "Arthur compton," *American Physical Society*, Dec 2005. [Online]. Available: https://www.aps.org/programs/outreach/history/historicsites/compton.cfm 1, 2

[2] A. H. Compton, "A quantum theory of the scattering of x-rays by light elements," *Phys. Rev.*, vol. 21, pp. 483–502, May 1923. [Online]. Available: https://link.aps.org/doi/10.1103/PhysRev.21.483 1

[3] G. Gilmore, *Practical Gamma-Ray Spectromtry*, 2008. 1, 2

[4] E. Browne, "Nuclear data sheets 108,2173," 2007. [Online]. Available: https://www.nndc.bnl.gov/nudat2/decaysearchdirect.jsp?nuc=137CS&unc=nds 3, 4

[5] M. S. Basunia, "Nuclear data sheets 127, 69," 2015. [Online]. Available: https://www.nndc.bnl.gov/nudat2/decaysearchdirect.jsp?nuc=22NA&unc=nds 5

[6] Y. Khazov, "Nuclear data sheets 112, 855," 2011. [Online]. Available: https://www.nndc.bnl.gov/nudat2/decaysearchdirect.jsp?nuc=133BA&unc=nds 5

[7] B. N. Taylor, "Fundamental constants: Electron mass," Mar 2019. [Online]. Available: https://physics.nist.gov/cgi-bin/cuu/Value?me 7

[8] S. M. Seltzer, "X-ray mass attenuation coefficients - ordinary concrete," 2004. [Online]. Available: https://physics.nist.gov/PhysRefData/XrayMassCoef/ComTab/concrete.html 8, 9

[9] R. Heath, "Computer techniques for the analysis of gamma-ray spectra obtained with nai and lithium-ion drifted germanium detectors," *Nuclear Instruments and Methods*, vol. 43, pp. 209–229, 08 1966. 8

[10] D. C. Radford, "Notes on the use of the program gf3," 2000. [Online]. Available: https://radware.phy.ornl.gov/gf3/gf3.html 8